

Effects of point defects on thermal and thermoelectric properties of InN

A. X. Levander,^{1,2} T. Tong,³ K. M. Yu,² J. Suh,^{1,2} D. Fu,^{1,4} R. Zhang,⁴ H. Lu,⁴
W. J. Schaff,⁵ O. Dubon,^{1,2} W. Walukiewicz,² D. G. Cahill,³ and J. Wu^{1,2,a)}

¹Department of Materials Science and Engineering, University of California, Berkeley, California 94720, USA

²Materials Sciences Division, Lawrence Berkeley National Laboratory, Berkeley, California 94720, USA

³Department of Materials Science and Engineering, University of Illinois, Urbana, Illinois 61801, USA

⁴Jiangsu Provincial Key Laboratory of Advanced Photonic and Electronic Materials, School of Electronic Science and Engineering, Nanjing University, Nanjing, Jiangsu 210093, People's Republic of China

⁵Department of Electrical and Computer Engineering, Cornell University, Ithaca, New York 14853, USA

(Received 19 November 2010; accepted 20 December 2010; published online 5 January 2011)

In contrast to most semiconductors, electrical conductivity of InN is known to increase upon high-energy particle irradiation. The effects of irradiation on its thermal and thermoelectric properties have yet to be investigated. Here we report the thermal conductivity of high-quality InN to be 120 W/m K and examine the effects of point defects generated by irradiation on the thermal conductivity and Seebeck coefficient. We show that irradiation can be used to modulate the thermal and thermoelectric properties of InN by controlling point defect concentrations. The thermoelectric figure of merit of InN was found to be insensitive to irradiation. © 2011 American Institute of Physics. [doi:10.1063/1.3536507]

The study of group III-nitrides is motivated by the wide band gap range of their alloys from the ultraviolet to the infrared ($E_{g,\text{AlN}}=6.1$ eV, $E_{g,\text{GaN}}=3.4$ eV, $E_{g,\text{InN}}=0.64$ eV), allowing for applications in a wide range of devices from optoelectronics to photovoltaics.¹ Since the discovery of the narrow band gap of InN from high-quality films in 2002, there has been vigorous research in the optoelectronic properties of InN and In-rich $\text{In}_{1-x}\text{Ga}_x\text{N}$ alloys.^{2,3} Measurements of the Seebeck coefficient of p-type InN have been used to determine hole concentrations by circumventing issues of surface Fermi level pinning in the conduction band.⁴ High-energy particle irradiation has been used to study the effects of point defects on the electrical and optoelectronic properties (e.g., carrier mobility and photoluminescence) of In-rich alloys.⁵

However, despite this vast progress, thermal properties of high-quality InN have not been investigated. The thermal conductivity of a material has become an increasingly important issue in the thermal management of high power and/or miniaturized devices. The cation/anion mass ratio of InN is the highest among all group III-V materials, which directly causes a wide phonon band gap and narrow acoustic phonon band in InN.¹ This high In/N mass ratio also implies a high sensitivity of its thermal conductivity to In-related point defects.⁶ In this work we examine the thermal and thermoelectric properties of InN and the effect of irradiation-introduced native point defects on these properties.

The single-crystal InN films examined in this study were grown by molecular-beam epitaxy on *c*-sapphire substrates with a GaN buffer layer.⁷ The 500–2100 nm thick InN layers were not intentionally doped. They have background electron concentrations between 8×10^{17} and 3×10^{18} cm⁻³ and mobilities between 1500 and 1045 cm²/V s. Their high mobilities and a strong photoluminescence peak at ~ 0.7 eV indicate high crystal quality and low impurity levels in these films.¹ The exact film thicknesses were determined by Ruth-

erford backscattering spectrometry with a 2.13 MeV He²⁺ beam. The irradiation was performed using a 2.13 MeV He²⁺ beam with current between 40 and 150 nA generated by a Pelletron tandem accelerator. The ion beam was defocused to an area of 40 mm² to cover the entire sample with doses ranging between 6.5×10^{13} and 1×10^{16} He²⁺/cm². Simulations using the stopping and range of ions in matter (SRIM) software predicted that the concentration of defects generated by the ion beam is relatively uniform (Fig. 1 inset), and the ions would penetrate the entire thickness of the InN film, leaving end of range damage in the sapphire substrate.⁸

Out-of-plane thermal conductivity measurements were conducted at room temperature using time-domain thermoreflectance (TDTR).⁹ Details of the measurement setup are described in Ref. 10. The modulation frequency of the pump

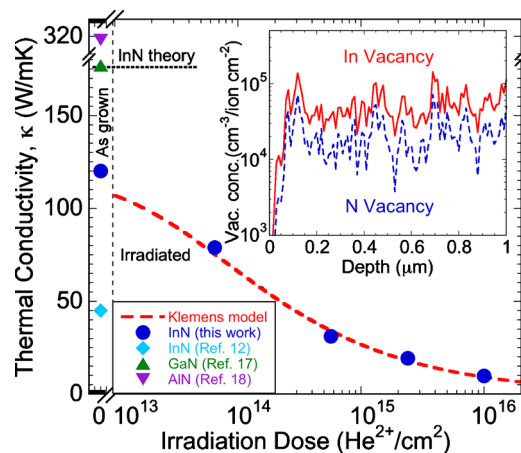


FIG. 1. (Color online) Thermal conductivity of InN as a function of He²⁺ irradiation dose compared to theoretical prediction from Eq. (1). A fitting parameter of $\beta=0.13$ was used to correlate the SRIM-predicted In point defect concentration and the actual phonon-scattering defect concentration. Previously reported thermal conductivities of GaN, AlN, and InN are included as a reference. Inset is SRIM calculated In and N vacancy concentration as a function of depth.

^{a)}Electronic mail: wuj@berkeley.edu.

beam was fixed at 10 MHz. The radii of the pump and probe beams were 15 μm at the sample surface and the total laser power of 30 mW caused a <5 K temperature increase. The samples were prepared for TDTR by coating the films with a ~ 100 nm thick magnetron sputtered Al film. Data analysis procedures are described in Ref. 11.

The thermal conductivity of the as-grown and irradiated films is plotted in Fig. 1. The pristine InN thermal conductivity was determined to be 120 W/m K along the c-axis direction, more than twice the previously reported 45 W/m K for InN grown by nitrogen microwave plasma chemical vapor deposition.¹² Our measured value is in better agreement with the theoretical lattice thermal conductivity of InN of ~ 180 W/m K at room temperature, calculated using $\kappa_{\text{theoretical}} = C_v l v / 3$, where C_v is the molar specific heat, v is the Debye-averaged acoustic phonon velocity along the c-axis, and $l = a / (\alpha_v \gamma T)$ is the phonon mean free path. The interatomic spacing a is half the c lattice parameter, α_v is the volume thermal expansion coefficient, and γ is the Grüneisen parameter.^{1,12–14} The thermal conductivity measured from high-quality films in this work is expected to be closer to the theoretically predicted value. Moreover, the averaged acoustic phonon velocity along the c-axis (out-of-plane) differs from that of the in-plane by only 2% (Ref. 14); therefore, the thermal conductivity is expected to be isotropic within the experimental error.

The thermal conductivity is rapidly reduced by irradiation, and the behavior can be explained using the Klemens model for point defect thermal resistance.⁶ For point defect dominated phonon scattering, the thermal conductivity is dependent on the concentration of point defects that create a mass difference at the lattice sites. This is described by a point defect scattering relaxation time, $\tau = 1 / A \omega^4$, where ω is the phonon frequency. The parameter A depends on the dominant type of defects, which for this study are point defects generated by displacement of atoms due to the impinging He^{2+} ions. For point defects, A is given by $C \Omega (3 \Delta M / M)^2 / 4 \pi v^3$, where C is the defect concentration per unit cell, Ω is the unit cell volume, and $\Delta M / M$ is the relative change in mass for one defect per unit cell. Although defect clusters can form through various defect reactions, their overall contribution to the thermal conductivity reduction is expected to be minimal due to their low concentration at the irradiation doses considered.^{15,16}

The general form of thermal conductivity at $k_B T > \hbar \omega_D / 3$ is approximated as⁶

$$\kappa(\omega_0) = \kappa_0 \frac{\omega_0}{\omega_D} \arctan\left(\frac{\omega_D}{\omega_0}\right), \quad (1)$$

where κ_0 is the pristine lattice thermal conductivity and $\hbar \omega_D / k_B = 660$ K is the Debye temperature.¹ $\omega_0 \propto 1 / \sqrt{A}$ and represents the frequency where the umklapp scattering and point defect scattering rates are equal. Both vacancy and interstitial point defects are formed during irradiation, which have the same $\Delta M / M$. Due to the small ΔM for nitrogen vacancies/interstitials and their lower concentration predicted by SRIM (Fig. 1 inset), indium vacancies and interstitials are considered the dominant cause of the thermal conductivity reduction.

A single fitting parameter, β , was used to determine the relation between the theoretically predicted number of point defects using the Monte Carlo method of SRIM and the con-

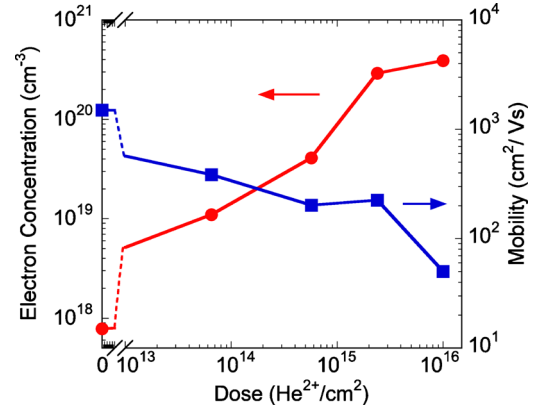


FIG. 2. (Color online) Free electron concentration and mobility of InN as a function of He^{2+} irradiation dose.

centration of defects required to account for the thermal conductivity reduction ($C_{\text{experimental}} = \beta C_{\text{SRIM}}$). The model fit shown in Fig. 1 was achieved using $\beta = 0.13$. The nonunity value of β can be caused by vacancy-interstitial annihilation that can occur both during and after irradiation and other effects from defect clusters not explicitly considered.¹⁵ SRIM only models a simple cumulative process that does not account for energetic bombardment that displaces an atom back to its original lattice position (dynamic annealing). A dynamical Monte Carlo simulation is needed for a more quantitative explanation of the nonunity value of β .

In Fig. 1 the thermal conductivity of InN is also compared to those of other group III-nitrides, GaN (177 W/m K) and AlN (319 W/m K).^{17,18} As expected, due to the heavier mass of the indium atom, and therefore the lower sound velocity of InN, the thermal conductivity of InN is the lowest of the three. We note that, even at the highest electrical conductivity ($\sigma \sim 3200 / \Omega \text{ cm}$), the electronic thermal conductivity is still much lower than the lattice thermal conductivity (estimated to be 1.7 W/m K from the Wiedemann–Franz law).

The electron concentration (n) and mobility (μ) of the InN films as characterized by Hall effect are shown in Fig. 2. As reported previously, the electron concentration of InN increases with native defect concentration due to its low-lying conduction band edge which makes native defects donorlike.¹⁹ The electron generation rate (R_e) for He^{2+} ions was determined to be $\sim 3500 \text{ cm}^{-1}$ based on a linear correlation between electron concentration and irradiation dose ($n = R_e \Phi$), which agrees well with previous reports of He^{2+} irradiation.²⁰ As expected, the mobility decreases with irradiation due to carrier scattering from these charged defects.

The Seebeck coefficient is plotted as a function of electron concentration in Fig. 3. In the degenerate doping limit, the Seebeck coefficient can be expressed as²¹

$$S_{\text{Degenerate}} = - \frac{k_B}{e} (r + 3/2) \frac{\pi^2}{3} \frac{k_B T}{\zeta}, \quad (2)$$

where ζ is the Fermi energy and r is the power law index relating the relaxation time to energy for free charge carriers ($\tau \propto \epsilon^r$). The nonparabolicity of the InN conduction band was taken into account in calculating the electron density dependence of ζ .¹ The model agrees reasonably well with the experimental data at electron concentrations greater than $\sim 10^{19} \text{ cm}^{-3}$ for which the degenerate approximation ap-

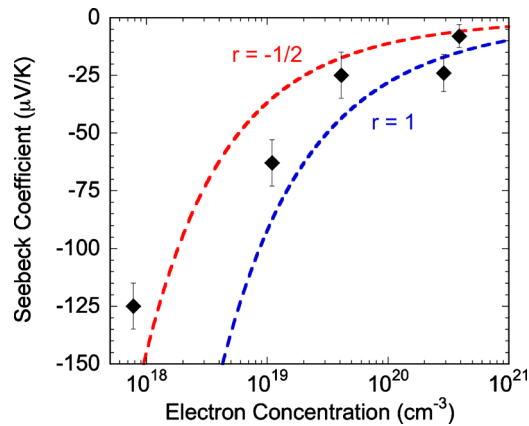


FIG. 3. (Color online) Seebeck coefficient of irradiated InN as a function of free electron concentration. The dashed lines are calculated from a nonparabolic band model of the Seebeck coefficient in the degenerate doping approximation with different r values.

plies. At low electron concentrations, the experimental data deviate from Eq. (2) due to breakdown of the degenerate doping approximation and a relatively larger contribution from electrons in the surface accumulation layer.²² The Seebeck coefficient was calculated using an r value of $-1/2$ or $+1$, which corresponds to electron scattering dominated by phonons or ionized impurities, respectively. The dependence of the Seebeck coefficient on irradiation-generated electrons is similar to previous studies of as-grown InN with variable electron concentrations.²³

The three thermoelectric parameters were used to calculate the thermoelectric figure of merit, $ZT = S^2 \sigma / \kappa$, as a function of irradiation dose. The ZT of this pristine sample was 0.007 and stayed within 30% of this value after the irradiation doses considered. The ZT of most materials typically decreases with irradiation due to a greatly reduced electrical conductivity.²⁴ InN is unique in that irradiation results in an increase in electrical conductivity in addition to the greatly reduced thermal conductivity. These positive contributions to ZT are not completely canceled by the lower Seebeck coefficient. This result suggests that in addition to being a radiation-resistant photovoltaic material,¹ the thermoelectric properties of InN are also radiation-resistant. Thermal annealing after the irradiation may affect S , σ , and κ differently and thus possibly enhance ZT .

In summary, we find high-energy ion irradiation to be a viable method for controlling the thermal, electrical, and thermoelectric properties of InN by introducing point defects. The thermal conductivity of high-quality InN was determined to be 120 W/m K, and the effects of point defects introduced by He²⁺ irradiation were examined. The Seebeck coefficient of the irradiated films agreed with the theoretically predicted values based on carrier concentration and ef-

fective mass. The thermoelectric figure of merit of InN was found to be insensitive to irradiation.

The materials processing and data analysis in this work were supported by the National Science Foundation (NSF) under Grant No. CBET-0932905. The irradiation work was supported by the Director, Office of Science, Office of Basic Energy Sciences, Materials Sciences and Engineering Division, of the U.S. Department of Energy under Contract No. DE-AC02-05CH11231. A.L. acknowledges a NSF graduate research fellowship. The TDTR measurement was supported by the Air Force Office of Scientific Research MURI Grant No. FA9550-08-1-0407. D. Fu and R. Zhang acknowledge support by Special Funds for Major State Basic Research Project of China (Grant No. 2011CB301901).

¹J. Wu, *J. Appl. Phys.* **106**, 011101 (2009).

²J. Wu, W. Walukiewicz, K. M. Yu, J. W. Ager III, E. E. Haller, H. Lu, W. J. Schaff, Y. Saito, and Y. Nanishi, *Appl. Phys. Lett.* **80**, 3967 (2002).

³*Indium Nitride and Related Alloys*, edited by T. D. Veal, C. F. McConville, and W. J. Schaff (CRC, Boca Raton, FL, 2010).

⁴N. Miller, J. W. Ager III, H. M. Smith III, M. A. Mayer, K. M. Yu, E. E. Haller, W. Walukiewicz, W. J. Schaff, C. Gallinat, G. Koblmüller, and J. S. Speck, *J. Appl. Phys.* **107**, 113712 (2010).

⁵K. M. Yu, *Phys. Status Solidi A* **206**, 1168 (2009).

⁶P. G. Klemens, *Phys. Rev.* **119**, 507 (1960).

⁷H. Lu, W. J. Schaff, J. Hwang, H. Wu, W. Yco, A. Pharkya, and L. F. Eastman, *Appl. Phys. Lett.* **77**, 2548 (2000).

⁸SRIM-2008, <http://www.srim.org/>.

⁹C. A. Paddock and G. L. Eesley, *J. Appl. Phys.* **60**, 285 (1986).

¹⁰D. G. Cahill, W. K. Ford, K. E. Goodson, G. D. Mahan, A. Majumdar, H. J. Maris, R. Merlin, and S. R. Phillpot, *J. Appl. Phys.* **93**, 793 (2003).

¹¹D. G. Cahill, *Rev. Sci. Instrum.* **75**, 5119 (2004).

¹²S. Krukowski, A. Witek, J. Adamczyk, J. Jun, M. Bockowski, I. Grzegory, B. Lucznik, G. Nowak, M. Wróblewski, A. Presz, S. Gierlotka, S. Stelmach, B. Palosz, S. Porowski, and P. Zinn, *J. Phys. Chem. Solids* **59**, 289 (1998).

¹³R. Berman, *Thermal Conduction in Solids* (Clarendon, Oxford, 1976), p. 47.

¹⁴A. Zubrilov, in *Properties of Advanced Semiconductor Materials GaN, AlN, InN, BN, SiC, SiGe*, edited by M. E. Levinstein, S. L. Rumyantsev, and M. S. Shur (Wiley, New York, 2001), pp. 49–66.

¹⁵J. S. Williams, *Mater. Sci. Eng., A* **253**, 8 (1998).

¹⁶D. P. White, *J. Appl. Phys.* **73**, 2254 (1993).

¹⁷J. Zou, D. Kotchetkov, A. A. Balandin, D. I. Florescu, and F. H. Pollak, *J. Appl. Phys.* **92**, 2534 (2002).

¹⁸G. Slack, R. A. Tanzilli, R. O. Pohl, and J. W. Vandersande, *J. Phys. Chem. Solids* **48**, 641 (1987).

¹⁹W. Walukiewicz, *Physica B* **302–303**, 123 (2001).

²⁰R. E. Jones, S. X. Li, L. Hsu, K. M. Yu, W. Walukiewicz, Z. Liliental-Weber, J. W. Ager III, E. E. Haller, H. Lu, and W. J. Schaff, *Physica B* **376–377**, 436 (2006).

²¹K. Seeger, *Semiconductor Physics* (Springer, New York, 2002).

²²J. W. L. Yim, R. E. Jones, K. M. Yu, J. W. Ager III, W. Walukiewicz, W. J. Schaff, and J. Wu, *Phys. Rev. B* **76**, 041303(R) (2007).

²³N. Miller, J. W. Ager III, R. E. Jones, H. M. Smith III, M. A. Mayer, K. M. Yu, M. E. Hawkrige, Z. Liliental-Weber, E. E. Haller, W. Walukiewicz, W. J. Schaff, C. Gallinat, G. Koblmüller, and J. S. Speck, *Physica B* **404**, 4862 (2009).

²⁴Th. Theilg, B. Heinz, and P. Ziemann, *J. Low Temp. Phys.* **105**, 933 (1996).